

# The chalcogenide compound $\text{Fe}_2\text{SnSe}_4$ : Synthesis and crystal structure analysis by powder X-ray diffraction

Pilar Delgado-Niño<sup>a</sup>, Cecilia Chacón<sup>b</sup>, Gustavo Marroquin<sup>c</sup>, Gerzon E. Delgado<sup>d\*</sup> 

<sup>a</sup>Universidad Libre, Facultad de Ingeniería, Bogotá, Colombia

<sup>b</sup>Centro de Tecnología para Aguas Profundas, Cátedras Conacyt-Instituto Mexicano del Petróleo, Veracruz, México

<sup>c</sup>Instituto Politécnico Nacional, Escuela Superior de Ingeniería Química e Industrias Extractivas, Ciudad de México, México

<sup>d</sup>Universidad de Los Andes, Departamento de Química, Facultad de Ciencias, Mérida, Laboratorio de Cristalografía, Venezuela

Received: April 05, 2020; Revised: October 11, 2020; Accepted: November 11, 2020

$\text{Fe}_2\text{SnSe}_4$  belongs to the adamantine family of quaternary chalcogenides crystallizing in the olivine type structure, which can be described from a hexagonal close-packing of selenium anions with the octahedral and tetrahedral sites occupied by the iron and tin cations, respectively. The structural characterization of the sample, synthesized by the melt and annealing technique, was carried out by powder X-ray diffraction at room temperature. The XRD data analysis shows, that  $\text{Fe}_2\text{SnSe}_4$  adopt the orthorhombic olivine type structure, space group  $Pnma$ , and unit cell parameters  $a = 13.2019(3)$  Å,  $b = 7.6746(1)$  Å,  $c = 6.3572(1)$  Å,  $V = 644.11(2)$  Å<sup>3</sup> were derived.

**Keywords:** Chalcogenides, Olivines, Chemical synthesis, Crystal structure, Powder X-ray diffraction, Rietveld refinement.

## 1. Introduction

The ternary chalcogenide semiconductors  $\text{A}^{\text{II}}\text{-B}^{\text{IV}}\text{-X}^{\text{VI}}_4$  (II= Mn, Fe, Co; IV= Si, Ge, Sn; VI= S, Se, Te) have drawn wide interest for their magnetic, optoelectronic and thermoelectric properties<sup>1-12</sup>. The presence of transition metal and chalcogenide elements in the same compound enables unique interaction between the electron spins, which is one of the factors that give rise to potential applications<sup>13</sup>.

These type of materials generally belongs to the adamantine family of ternary chalcogenide crystallizing in the olivine type structure<sup>1</sup> with the anions forming a hexagonal close packing and the cations in tetrahedral and octahedral coordination. However, a distorted spinel structure with space group  $I4_1/a$  has been reported for  $\text{Fe}_2\text{SnS}_4$ <sup>2</sup>, and an orthorhombic structure with space group  $Cmmm$  for  $\text{Mn}_2\text{SnS}_4$ <sup>3</sup>. It should be noted that the presence of a transition metal in these materials additionally introduces a magnetic behavior<sup>4</sup>.

From the point of view of their magnetic structure and properties, the chalcogenide olivines represent interesting examples of frustrated lattices of magnetic atoms determining complex magnetic excitations<sup>14</sup>. Materials belonging to this family of olivine-type compounds have been considered as good model systems to study multicritical phenomena<sup>15</sup>, and have found important new applications also for thermoelectric power generation<sup>8</sup>, and as cathode materials for batteries<sup>16</sup>.

In particular, for olivine-like structures containing iron atoms, recently it has been proven that the ternary chalcogenides  $\text{Fe}_2\text{GeS}_4$  and  $\text{Fe}_2\text{SiS}_4$  have the potential to overcome the

limitations in the binary  $\text{FeS}_2$ , which is considered as one of the promising light-absorbing material with high absorption coefficient to be used in thin film solar cells<sup>17</sup>. These materials are proposed to have high absorption coefficients and gap of 1.40 eV and 1.55 eV, respectively, which is more suitable for solar light absorption. Besides both phases are predicted to be more stable than the binary  $\text{FeS}_2$  phase. These properties make  $\text{Fe}_2\text{GeS}_4$  and  $\text{Fe}_2\text{SiS}_4$  as a potential material to use in photovoltaics<sup>17</sup>. Meanwhile, Fe-content olivine compounds with Se ad Te anions emerge as promising candidates with good thermoelectric performances<sup>8</sup>.

The compound  $\text{Fe}_2\text{SnSe}_4$ , or more precisely  $\text{Fe}_2\text{Sn}[\ ]\text{Se}_4$ , where  $[ ]$  denotes the cation vacancy which is included to maintain the same number of cations and anions sites, belongs to this family,  $\text{II}_2\text{-IV-VI}_4$ , of ternary chalcogenide semiconductors<sup>18</sup>. As regards to the physical properties of the ternary  $\text{Fe}_2\text{SnSe}_4$ , it was reported that it shows ferromagnetic behavior with a Curie temperature near to room temperature  $T_c = 301.4\text{K}$ <sup>5</sup>, and interesting transport properties for thermoelectric applications<sup>8</sup>. However, no complete X-ray crystal structure analysis has been reported and the only crystallographic information are the cell parameters: ( $a = 14.778$  Å,  $b = 10.764$  Å,  $c = 6.061$  Å,  $V = 964.0$  Å<sup>3</sup>)<sup>5</sup> and ( $a = 14.803$  Å,  $b = 10.768$  Å,  $c = 6.059$  Å,  $V = 965.8$  Å<sup>3</sup>)<sup>9</sup>. Moreover, a search in the databases Powder Diffraction File PDF-ICDD<sup>19</sup>, Inorganic Crystal Structure Database (ICSD)<sup>20</sup>, and Springer Materials<sup>21</sup> showed no entries for this ternary chalcogenide compound.

It is very important to establish the crystal structure of a semiconductor because this is used to understand and explain

\*e-mail: gerzon@ula.ve

the physical properties relevant to possible applications. In the hope of providing a full description of the  $\text{Fe}_2\text{SnSe}_4$  structure, in the present work, and as part of ongoing crystal structural studies on chalcogenide compounds<sup>22-27</sup>, we report the structural characterization of this ternary compound using powder X-ray diffraction techniques.

## 2. Experimental procedures

### 2.1 Synthesis

$\text{Fe}_2\text{SnSe}_4$  was synthesized by the reaction of high purity elements, Fe, Sn, and Se with a nominal purity of at least 99.99% (Sigma-Aldrich), using the melt and annealing technique. Stoichiometric quantities of the three elements were charged in an evacuated quartz ampoule, previously subject to pyrolysis to avoid reaction of the starting materials with quartz. Then, the ampoule was sealed under vacuum ( $\sim 10^{-4}$  Torr) and the fusion process was carried out inside a furnace (vertical position) heated up to 1100 K at a rate of 20 K/h, with a stop of 48 h at 493 K (melting point of Se). The ampoule was shaking using a mechanical system during all the heating process to guarantee the complete mixing of all the elements. Then, the temperature was gradually decreased until 600 K and this temperature was maintained for 30 days. Finally, the furnace was turned off and the ingots were cooled to room temperature.

### 2.2 Chemical analysis

The stoichiometry of the sample was determined by energy-dispersive X-ray spectroscopy (EDS) analysis using a JMS-6400 scanning electron microscope (SEM). The average composition of Fe: Sn: Se sample, taken from the central part of the ingots, was 14.0: 28.6: 57.4 at. % that led to the formula close to the ideal value composition 2: 1: 4. The error in the standardless analysis was around 5%.

### 2.3 X-ray powder diffraction

For the X-ray analysis, a small quantity of the sample was ground mechanically in an agate mortar and pestle. The resulting fine powder was mounted on a flat holder. The X-ray powder diffraction data were collected at room temperature, in reflection mode using a Panalytical X'pert diffractometer using  $\text{CuK}\alpha$  radiation ( $\lambda = 1.5418 \text{ \AA}$ ). The specimen was scanned from 10 to  $80^\circ 2\theta$ , with a step size of  $0.02^\circ$  and counting time of 20 s. Silicon (SRM-640) was used as an external standard.

## 3. Results and Discussion

For pattern indexing and unit cell parameter refinement, the precise determination of peaks positions was carried out using the Highscore Plus v3.0 analytical software. The X-ray diffractogram of  $\text{Fe}_2\text{SnSe}_4$  is shown in Figure 1. A search in the PDF-ICDD database<sup>19</sup> was performed and no binaries are present. Therefore, the powder X-ray pattern corresponds to a single phase.

The 20 first measured reflections were completely indexed using the program DICVOL04<sup>28</sup>, which gave a unique solution in an orthorhombic cell with unit cell parameters  $a = 13.202 \text{ \AA}$ ,  $b = 7.675 \text{ \AA}$ ,  $c = 6.357 \text{ \AA}$ , and indexed figures of merit  $M_{20} = 26.7^{29}$  and  $F_{20} = 40.7(0.0100, 49)^{30}$ . Systematic absences indicate a  $P$ -type cell, which suggested along with the sample composition and cell parameter dimensions that this material is isostructural with the olivine type compounds with orthorhombic space group  $Pnma$  ( $N^\circ 62$ ) as the recently reported compound  $\text{Mn}_2\text{SnSe}_4$  [27]. So the space group  $Pnma$  and the atomic position parameters of  $\text{Mn}_2\text{SnSe}_4$  were taken as the starting values to refine the structural parameters of  $\text{Fe}_2\text{SnSe}_4$ .

The crystal structure refinement, employing the Rietveld method<sup>31</sup>, was performed using the Fullprof program<sup>32</sup> available in the software package Winplotr<sup>33</sup>.

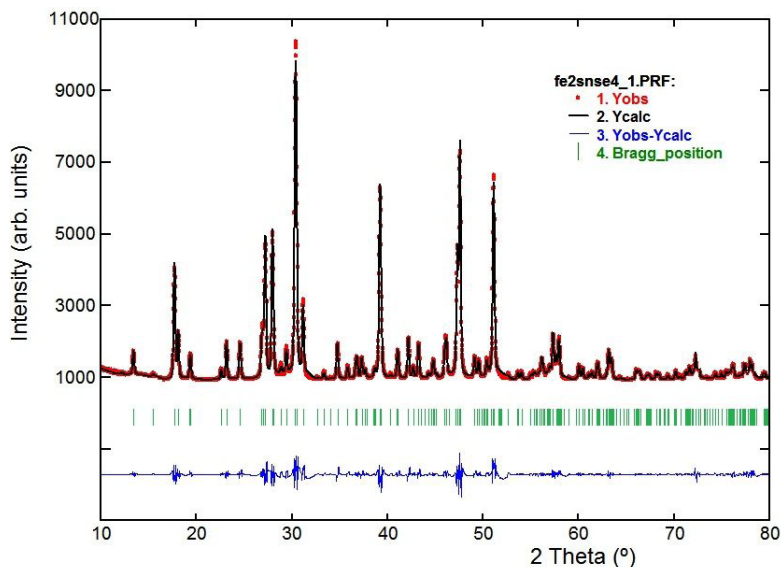


**Figure 1.** Observed (circles), calculated (solid line), and difference plot of the final Rietveld refinement of  $\text{Fe}_2\text{SnSe}_4$ . The Bragg reflections are indicated by vertical bars.

The indexing results were taken as the starting unit cell parameters. The angular dependence of the peak full width at half maximum (FWHM) was described by the Caglioti's formula,  $FWHM^2 = U \tan^2 \theta + V \tan \theta + W$ , where  $U$ ,  $V$ , and  $W$  are fitting parameters<sup>34</sup>. Peak shapes were described by the parameterized Thompson-Cox-Hastings pseudo-Voigt profile function<sup>35</sup>. The background was described by the automatic interpolation of 66 points throughout the whole pattern. The thermal motion of the atoms was described by one overall isotropic temperature factor. Details of the Rietveld refinement of Fe<sub>2</sub>SnSe<sub>4</sub> are summarized in Table 1, and the atomic positions and thermal displacement factors are presented in Table 2. The observed, calculated, and residual powder XRD patterns of Fe<sub>2</sub>SnSe<sub>4</sub> are shown in Figure 1.

It should be noted that the previously reported unit cell parameters for this material<sup>5,9</sup> will be used to reproduce the experimental diffraction pattern, however, it does not produce good results. On the other hand, the unit cell volume obtained in this work agrees in the order of magnitude with those reported for similar compounds (see Table 3).

The structure of the ternary chalcogenide Fe<sub>2</sub>SnSe<sub>4</sub> can be described as an olivine type structure which consists of a hexagonal close packing of Se<sup>2-</sup> anions with the Fe<sup>+2</sup> cations

occupying half of the octahedral sites and the Sn<sup>+4</sup> cations occupying an eighth of the tetrahedral sites. As expected for these materials each anion is coordinated by four cations (three Fe and one Sn) located at the corners of a slightly distorted tetrahedron. The polyhedral coordination of the cations and anions are presented in Figure 2, showing the FeSe<sub>6</sub> octahedra, SnSe<sub>4</sub> tetrahedra and Se(SnFe<sub>3</sub>) tetrahedra formed. Figure 3 shows the unit cell diagram of Fe<sub>2</sub>SnSe<sub>4</sub> with the octahedra and tetrahedra coordination around the cations. Details of the olivine type structure description are published elsewhere<sup>21</sup>.

Unit cell parameter values of Fe<sub>2</sub>SnSe<sub>4</sub> are very similar to those reported in the crystal structures of the Fe-content compounds with II<sub>2</sub>-IV-VI<sub>4</sub> compositions as shown in Table 3. The Fe-Se bond distances vary from 2.52(1) Å to 2.76(2) Å [with a mean value of 2.66(2) Å] and Sn-Se bond distances from 2.42(1) Å to 2.56(2) Å [mean value of 2.47(2) Å]. These interatomic distances are shorter than the sum of the respective ionic radii for structures tetrahedrally bonded<sup>36</sup>, nevertheless compare quite well with those observed in other adamantane structures with common elements, found in the Inorganic Crystal Structure Database (ICSD)<sup>20</sup>, such as Cu<sub>2</sub>FeSnSe<sub>4</sub><sup>37</sup>, Fe<sub>2</sub>GeSe<sub>4</sub><sup>38</sup>, Cu<sub>2</sub>(Cd,Zn)SnSe<sub>4</sub><sup>39</sup>, Cu<sub>2</sub>SnSe<sub>4</sub><sup>40</sup>,

**Table 1.** Rietveld refinement details for the ternary chalcogenide Fe<sub>2</sub>SnSe<sub>4</sub>.

molecular formula	Fe <sub>2</sub> SnSe <sub>4</sub>	wavelength (CuK <sub>α</sub> )	1.5418 Å
molecular weight (g/mol)	546.24	data range 2θ (°)	10-80
<i>a</i> (Å)	13.2019(3)	step size 2θ (°)	0.02
<i>b</i> (Å)	7.6746(1)	counting time (s)	20
<i>c</i> (Å)	6.3572(1)	step intensities	4001
<i>V</i> (Å <sup>3</sup> )	644.11(2)	Peak-shape profile	pseudo-voigt
<i>Z</i>	4	R <sub>p</sub> (%)	6.1
Crystal system	orthorhombic	R <sub>wp</sub> (%)	6.5
Space group	<i>Pnma</i> (N° 62)	R <sub>exp</sub> (%)	5.5
<i>d</i> <sub>calc</sub> (g/cm <sup>3</sup> )	5.63	R <sub>B</sub> (%)	5.0
Temperature (K)	298(1)	<i>S</i>	1.2

$R_{exp} = 100 [(N-P+C) / \sum_w (y_{obs}^2)]^{1/2}$ ;  $R_p = 100 \sum |y_{obs} - y_{calc}| / \sum |y_{obs}|$ ;  $R_{wp} = 100 [\sum_w |y_{obs} - y_{calc}|^2 / \sum_w |y_{obs}|^2]^{1/2}$ ;  $S = [R_{wp} / R_{exp}]$ ;  $R_B = 100 \sum_k |I_k - I_{calc}| / \sum_k |I_k|$ ;  $N-P+C$  is the number of degrees of freedom

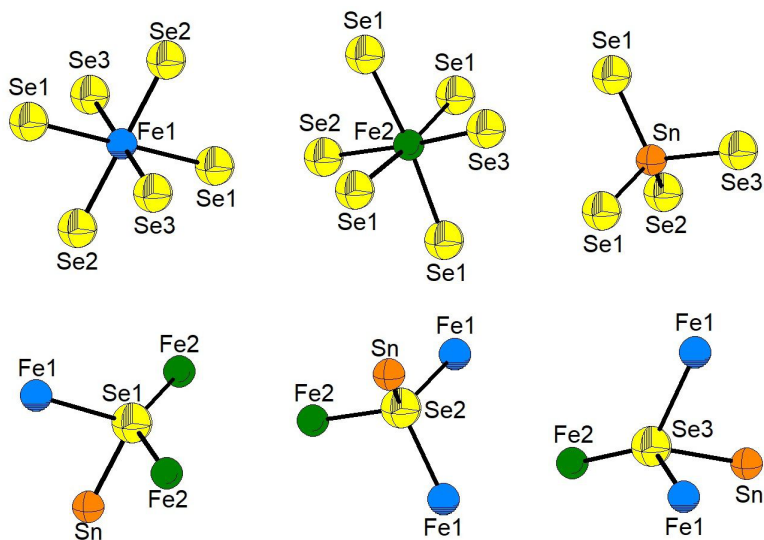
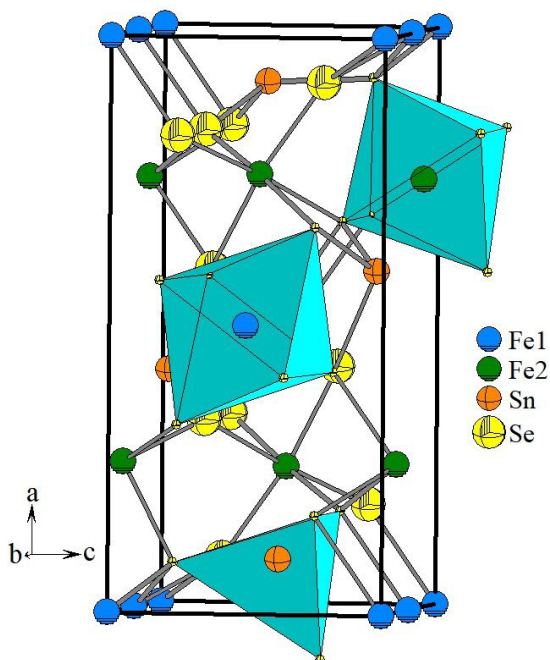
**Table 2.** Atomic coordinates, occupancy factors, isotropic temperature factors, and geometric parameters (Å, °) for Fe<sub>2</sub>SnSe<sub>4</sub>.

Atom	Ox.	Site	<i>x</i>	<i>y</i>	<i>z</i>	foc	B <sub>iso</sub> (Å <sup>2</sup> )
Fe1	+2	4 <i>a</i>	0	0	0	1	0.6(2)
Fe2	+2	4 <i>c</i>	0.242(1)	¼	0.503(1)	1	0.6(2)
Sn	+4	4 <i>c</i>	0.407(1)	¼	0.073(1)	1	0.6(2)
Se1	-2	8 <i>d</i>	0.328(1)	0.008(1)	0.253(1)	1	0.6(2)
Se2	-2	4 <i>c</i>	0.416(2)	¼	0.688(2)	1	0.6(2)
Se3	-2	4 <i>c</i>	0.583(2)	¼	0.247(1)	1	0.6(2)
Fe1-Se1 <sup>ii</sup>	2.76(1)	Fe1-Se2 <sup>iii</sup>	2.52(1)	Fe1-Se3 <sup>iv</sup>	2.73(1)		
Fe2-Se1 <sup>v</sup>	2.70(1)	Fe2-Se1	2.70(1)	Fe2-Se2	2.57(2)		
Sn-Se1	2.42(1)	Sn-Se2 <sup>i</sup>	2.45(1)	Sn-Se3	2.56(2)		
Se1 <sup>iv</sup> -Fe1-Se2 <sup>iii</sup>	96.5(2)	Se3 <sup>iii</sup> -Fe2-Se1 <sup>vi</sup>	89.0(2)	Se2 <sup>i</sup> -Sn-Se3	113.1(4)		
Se1 <sup>iv</sup> -Fe1-Se3 <sup>iv</sup>	88.6(2)	Se3 <sup>iii</sup> -Fe2-Se1	89.0(2)	Se2 <sup>i</sup> -Sn-Se1 <sup>vi</sup>	119.4(2)		
Se1 <sup>iv</sup> -Fe1-Se3 <sup>iii</sup>	91.4(2)	Se3 <sup>iii</sup> -Fe2-Se1 <sup>vii</sup>	94.6(2)	Se2 <sup>i</sup> -Sn-Se1	119.4(2)		
Se1 <sup>iv</sup> -Fe1-Se2 <sup>iv</sup>	83.5(2)	Se3 <sup>iii</sup> -Fe2-Se1 <sup>v</sup>	94.6(2)	Se1 <sup>vi</sup> -Sn-Se3	100.6(3)		
Se1 <sup>iv</sup> -Fe1-Se1 <sup>ii</sup>	180.0(3)	Se1 <sup>vi</sup> -Fe2-Se1 <sup>v</sup>	174.8(2)	Se1 <sup>vi</sup> -Sn-Se1	100.4(3)		
Se2 <sup>iii</sup> -Fe1-Se2 <sup>iv</sup>	180.0(5)	Se1-Fe2-Se1 <sup>viii</sup>	174.8(2)	Se3-Sn-Se1	100.4(3)		

Symmetry codes: (i) *x*, *y*, -1+*z*; (ii) -0.5+*x*, *y*, 0.5-*z*; (iii) -0.5+*x*, 0.5-*y*, 0.5-*z*; (iv) 0.5-*x*, -*y*, -0.5+*z*; (v) 0.5-*x*, -*y*, 0.5+*z*; (vi) *x*, 0.5-*y*, *z*; (vii) 0.5-*x*, 0.5+*y*, 0.5+*z*.

**Table 3.** Crystallographic information reported in the literature for the system  $\text{Fe}_2\text{-IV-VI}_4$  (IV= Si, Ge, Sn; VI= S, Se, Te).

Compound	SG	<i>a</i> (Å)	<i>b</i> (Å)	<i>c</i> (Å)	<i>V</i> (Å <sup>3</sup> )	Ref.
$\text{Fe}_2\text{SnS}_4$	<i>I4<sub>v</sub>/d</i>	7.308(5)	7.308(5)	10.338(9)	552.1(3)	[2]
$\text{Fe}_2\text{SiS}_4$	<i>Pnma</i>	12.407(2)	7.198(1)	5.812(1)	519.0(1)	[1]
$\text{Fe}_2\text{GeS}_4$	<i>Pnma</i>	12.467(2)	7.213(1)	5.902(1)	530.7(2)	[1]
$\text{Fe}_2\text{GeSe}_4$	<i>Pnma</i>	13.069(1)	7.559(1)	6.2037(6)	612.8(1)	[34]
$\text{Fe}_2\text{GeTe}_4$	<i>Pnma</i>	13.655(2)	7.898(1)	6.484(1)	699.3(2)	[7]
$\text{Fe}_2\text{SnSe}_4$	<i>Pnma</i>	13.2019(3)	7.6746(1)	6.3572(1)	644.11(2)	this work

**Figure 2.** Coordination polyhedra of the cations (Fe1, Fe2, Sn) and anions (Se), showing the  $\text{FeSe}_6$  octahedra,  $\text{SnSe}_4$  tetrahedra, and  $\text{Se}(\text{SnFe}_3)$  tetrahedra formed in the  $\text{Fe}_2\text{SnSe}_4$  structure.**Figure 3.** Unit cell diagram in the *ac* plane of the olivine type compound  $\text{Fe}_2\text{SnSe}_4$  (*Pnma*) showing the  $\text{FeSe}_6$  octahedra and  $\text{SnSe}_4$  tetrahedra.

$\text{Cu}_2\text{SnSe}_3$ <sup>41</sup>,  $\text{Fe}_2\text{CrSe}_4$ <sup>42</sup>,  $\text{Cu}_2\text{MnSnSe}_4$ <sup>43</sup>,  $\text{CuFe}(\text{Al}, \text{In}, \text{Ga})\text{Se}_3$ <sup>44,45</sup> and  $\text{CuFe}_2(\text{Al}, \text{Ga}, \text{In})\text{Se}_4$ <sup>46,47</sup>. All the bond angles in the structure of  $\text{Fe}_2\text{SnSe}_4$  are close to the ideal tetrahedral and octahedral bond angle values.

## 4. Conclusions

The crystal structure of the ternary magnetic compound  $\text{Fe}_2\text{SnSe}_4$  was refined using powder X-ray diffraction through the Rietveld method. This material was synthesized by the melt and annealing technique and crystallizes with an olivine structure in the orthorhombic space group *Pnma*. This is a new compound of the  $\text{II}_2\text{-IV-VI}_4$  family of semiconductors with an olivine-type structure. The crystal structure knowledge of  $\text{Fe}_2\text{SnSe}_4$  allows further investigation of this material about their structure-property relationship. This ternary semiconductor compound can be considered as a potential candidate for device thermoelectric applications.

## 5. Acknowledgments

This work was supported by FONACIT (Grant LAB-97000821).

## 6. References

- Vincent H, Bertaut EF, Baur WH, Shannon RD. Polyhedral deformations in olivine-type compounds and the crystal structure

- of  $\text{Fe}_2\text{SiS}_4$  and  $\text{Fe}_2\text{GeS}_4$ . *Acta Crystallogr B*. 1976;32(6):1749-55. <http://dx.doi.org/10.1107/S056774087600633X>.
2. Jumas JC, Philippot E, Maurin M. Etude structurale d'un thiospinelle d'étain  $\text{Fe}_2\text{SnS}_4$ . *Acta Crystallogr B*. 1977;33(12):3850-4. <http://dx.doi.org/10.1107/S0567740877012205>.
  3. Wintenberger M, Jumas JC. Etude par diffraction neutronique de  $\text{Mn}_2\text{SnS}_4$ : affinement de la structure cristallographique et détermination de la structure magnétique. *Acta Crystallogr B*. 1980;36(9):1993-6. <http://dx.doi.org/10.1107/S0567740880007789>.
  4. Lamarche G, Lamarche F, Lamarche AM. A possible 83K magnetic detector for high energy particles. *Physica B*. 1994;194-196:219-20. [http://dx.doi.org/10.1016/0921-4526\(94\)90439-1](http://dx.doi.org/10.1016/0921-4526(94)90439-1).
  5. Quintero M, Ferrer D, Caldera D, Moreno E, Quintero E, Morocoima M, et al. Lattice parameter values and magnetic properties for the  $\text{Mn}_2\text{GeTe}_4$ ,  $\text{Fe}_2\text{GeTe}_4$ , and  $\text{Fe}_2\text{SnSe}_4$  compounds. *J Alloys Compd*. 2009;469(1-2):4-8. <http://dx.doi.org/10.1016/j.jallcom.2008.01.096>.
  6. Quintero M, Quintero E, Caldera D, Moreno E, Morocoima M, Grima P, et al. Magnetic properties for the  $\text{Mn}_2\text{GeTe}_4$  compound. *J Magn Magn Mater*. 2009;321(4):291-9. <http://dx.doi.org/10.1016/j.jmmm.2008.09.003>.
  7. Delgado GE, Betancourt L, Mora AJ, Contreras JE, Grima-Gallardo P, Quintero M. Synthesis and crystallographic study of the ternary compound  $\text{Fe}_2\text{GeTe}_4$ . *Chalcogenide Lett* [serial on the Internet]. 2010 [cited 2020 July 3];7:133-8. Available from: [http://chalcogen.ro/133\\_Delgado.pdf](http://chalcogen.ro/133_Delgado.pdf)
  8. Gudelli VK, Kanchana V, Vaitheeswaran G. Predicted thermoelectric properties of olivine-type  $\text{Fe}_2\text{GeCh}_4$  ( $\text{Ch}=\text{S}$ ,  $\text{Se}$  and  $\text{Te}$ ). *J Phys Condens Matter*. 2016;28(2):025502. <http://dx.doi.org/10.1088/0953-8984/28/2/025502>.
  9. Wei K, Martin J, Nolas GS. Synthesis and transport properties of  $\text{Fe}_2\text{SnSe}_4$ . *J Alloys Compd*. 2018;732:218-21. <http://dx.doi.org/10.1016/j.jallcom.2017.10.202>.
  10. Nagai H, Hayashi K, Miyazaki Y. Thermoelectric properties of olivine-type sulfides  $\text{Tm}_2\text{X}_2\text{S}_4$  ( $\text{Tm}=\text{Mn}$ ,  $\text{Fe}$ ,  $\text{X}=\text{Si}$ ,  $\text{Ge}$ ). *Trans Mater Res Soc Jpn*. 2018;43(1):13-7. <http://dx.doi.org/10.14723/tmrj.43.13>.
  11. Davydova A, Eriksson J, Chen R, Rudisch K, Persson C, Scragg JJS. Thio-olivine  $\text{Mn}_2\text{SiS}_4$  thin films by reactive magnetron sputtering: structural and optical properties with insights from first principles calculations. *Mater Des*. 2018;152:110-8. <http://dx.doi.org/10.1016/j.matdes.2018.04.080>.
  12. Solzi M, Pernechele C, Attolini G, Delgado GE, Sagredo V. Magnetic ordering of  $\text{Mn}_2\text{GeS}_4$  single crystals with olivine structure. *J Magn Magn Mater*. 2020;497:166164. <http://dx.doi.org/10.1016/j.jmmm.2019.166164>.
  13. Jungwirth T, Sinova J, Masek J, Kucera J, MacDonald AH. Theory of ferromagnetic (III, Mn) V semiconductors. *Rev Mod Phys*. 2006;78(3):809-64. <http://dx.doi.org/10.1103/RevModPhys.78.809>.
  14. Hagemann IS, Khalifah PG, Ramirez AP, Cava RJ. Geometric magnetic frustration in olivines. *Phys Rev B Condens Matter Mater Phys*. 2000;62(2):R771-4. <http://dx.doi.org/10.1103/PhysRevB.62.R771>.
  15. Mikus H, Deiseroth HJ, Aleksandrov K, Ritter C, Kremer RK. The magnetic structure of  $\text{Mn}_2\text{GeSe}_4$ . *Eur J Inorg Chem*. 2007;2007(11):1515-8. <http://dx.doi.org/10.1002/ejic.200600770>.
  16. Torres A, Arroyo de Dompablo ME. Comparative Investigation of  $\text{MgMnSiO}_4$  and Olivine-Type  $\text{MgMnSiS}_4$  as Cathode Materials for Mg Batteries. *J Phys Chem C*. 2018;122(17):9356-62. <http://dx.doi.org/10.1021/acs.jpcc.8b02369>.
  17. Yu L, Lany S, Kykyneshi R, Jieratum V, Ravichandran R, Pelatt B, et al. Iron chalcogenide photovoltaic absorbers. *Adv Energy Mater*. 2011;1(5):748-53. <http://dx.doi.org/10.1002/aenm.201100351>.
  18. Parthé E. Wurtzite and zinc-blende structures. In: Westbrook JH, Fleischer RL, editors. *Intermetallic compounds, principles and practices*. Chichester: John Wiley & Sons; 1995. (vol. 1).
  19. International Centre for Diffraction Data. PDF-ICDD-Powder Diffraction File (Set 1-69). Newtown Square: International Centre for Diffraction Data; 2017.
  20. Gemlin Institute. ICSD - Inorganic Crystal Structure Database: scientific manual [Internet]. Karlsruhe: Gemlin Institute; 2008 [cited 2020 July 3]. Available from: [https://www.nist.gov/sites/default/files/documents/srd/09-0303-sci\\_man\\_ICSD\\_v1.pdf](https://www.nist.gov/sites/default/files/documents/srd/09-0303-sci_man_ICSD_v1.pdf)
  21. SpringerMaterials [Internet]. 2020 [cited 2020 July 3]. Available from: <https://materials.springer.com>
  22. Delgado GE, Manfredy L, López-Rivera SA. Crystal structure of the ternary semiconductor  $\text{Cu}_2\text{In}_{4/3}\text{Te}_{4/3}\text{Se}_8$  determined by X-ray powder diffraction data. *Powder Diffr*. 2018;33(3):237-41. <http://dx.doi.org/10.1017/S0885715618000519>.
  23. Marroquín G, Delgado GE, Grima-Gallardo P, Quintero M. Structural characterization of the new diamond-like semiconductor  $\text{CuVInSe}_3$ . *Rev Mex Fis*. 2018;64(6):548. <http://dx.doi.org/10.31349/RevMexFis.64.548>.
  24. Delgado GE, Sagredo V. Synthesis and crystal structure of the quaternary semiconductor  $\text{Cu}_2\text{NiGeS}_4$ , a new stannite-type compound. *Rev Mex Fis*. 2019;65:355-9. <http://dx.doi.org/10.31349/RevMexFis.65.355>.
  25. Delgado GE, Rincón C, Marroquín G. On the crystal structure of the ordered vacancy compound  $\text{Cu}_3\text{In}_2\text{Te}_9$ . *Rev Mex Fis*. 2019;65:360-4. <http://dx.doi.org/10.31349/RevMexFis.65.360>.
  26. Delgado-Niño P, Chacón C, Delgado GE. A new ordered vacancy compound; preparation and crystal structure of  $\text{Ag}_3\text{In}_2\text{Te}_9$ . *Rev Mex Fis*. 2019;65:475-8. <http://dx.doi.org/10.31349/RevMexFis.65.475>.
  27. Chacón C, Delgado-Niño P, Delgado GE. Synthesis and crystal structure determination of the new olivine-type compound  $\text{Mn}_2\text{SnSe}_4$ . *Rev Mex Fis*. 2019;66(1):30-4. <http://dx.doi.org/10.31349/RevMexFis.66.30>.
  28. Boulfif A, Löuer D. Powder pattern indexing with the dichotomy method. *J Appl Cryst*. 2004;37(5):724-31. <http://dx.doi.org/10.1107/S0021889804014876>.
  29. de Wolff PM. A simplified criterion for the reliability of a powder pattern indexing. *J Appl Cryst*. 1968;1(2):108-13. <http://dx.doi.org/10.1107/S002188986800508X>.
  30. Smith GS, Snyder RLFN. A criterion for rating powder diffraction patterns and evaluating the reliability of powder pattern indexing. *J Appl Cryst*. 1979;12(1):60-5. <http://dx.doi.org/10.1107/S002188987901178X>.
  31. Rietveld HM. A profile refinement method for nuclear and magnetic structures. *J Appl Cryst*. 1969;2(2):65-71. <http://dx.doi.org/10.1107/S0021889869006558>.
  32. Rodríguez-Carvajal J. Recent advances in magnetic structure determination by neutron powder diffraction. *Physica B*. 1993;192(1-2):55-69. [http://dx.doi.org/10.1016/0921-4526\(93\)90108-1](http://dx.doi.org/10.1016/0921-4526(93)90108-1).
  33. Roisnel T, Rodríguez-Carvajal J. WinPLOTR: a windows tool for powder diffraction pattern analysis. *Mater Sci Forum*. 2001;378-381:118-24. <http://dx.doi.org/10.4028/www.scientific.net/MSF.378-381.118>.
  34. Caglioti G, Paoletti A, Ricci FP. Choice of collimators for a crystal spectrometer for neutron diffraction. *Nucl Instrum*. 1958;3(4):223-8. [http://dx.doi.org/10.1016/0369-643X\(58\)90029-X](http://dx.doi.org/10.1016/0369-643X(58)90029-X).
  35. Thompson P, Cox DE, Hastings JB. Rietveld refinement of Debye-Scherrer synchrotron X-ray data from  $\text{Al}_2\text{O}_3$ . *J Appl Cryst*. 1987;20(2):79-83. <http://dx.doi.org/10.1107/S0021889887087090>.
  36. Shannon RS. Revised effective ionic radii and systematic studies of interatomic distances in halides and chalcogenides. *Acta Crystallogr A*. 1976;32(5):751-67. <http://dx.doi.org/10.1107/S0567739476001551>.
  37. Roque-Infante E, Delgado JM, López-Rivera SA. Synthesis and crystal structure of  $\text{Cu}_2\text{FeSnSe}_4$ , a  $\text{I}_2\text{IIIIVVI}_4$  semiconductor. *Mater Lett*. 1997;33(1-2):67-70. [http://dx.doi.org/10.1016/S0167-577X\(97\)00079-7](http://dx.doi.org/10.1016/S0167-577X(97)00079-7).

38. Henao JA, Delgado JM, Quintero M. X-ray powder diffraction data and structural study of  $\text{Fe}_2\text{GeSe}_4$ . *Powder Diffr.* 1998;13(4):196-201. <http://dx.doi.org/10.1017/S0885715600010101>.
39. Olekseyuk ID, Gulay LD, Dydchak IV, Piskach LV, Parasyuk OV, Marchuk OV. Single crystal preparation and crystal structure of the  $\text{Cu}_2\text{Zn/Cd,Hg/SnSe}_4$  compounds. *J Alloys Compd.* 2002;340(1-2):141-5. [http://dx.doi.org/10.1016/S0925-8388\(02\)00006-3](http://dx.doi.org/10.1016/S0925-8388(02)00006-3).
40. Marcano G, Rincón C, Marín G, Tovar R, Delgado GE. Crystal growth and characterization of the cubic semiconductor  $\text{Cu}_2\text{SnSe}_4$ . *J Appl Phys.* 2002;92(4):1811-5. <http://dx.doi.org/10.1063/1.1492018>.
41. Delgado GE, Mora AJ, Marcano G, Rincón C. Crystal structure refinement of the semiconducting compound  $\text{Cu}_2\text{SnSe}_3$  from X-ray powder diffraction data. *Mater Res Bull.* 2003;38(15):1949-55. <http://dx.doi.org/10.1016/j.materresbull.2003.09.017>.
42. Delgado GE, Sagredo V. Crystal structure of the  $\text{Fe}_2\text{CrSe}_4$  compound from X-ray powder diffraction. *Phys Status Solidi.* 2004;201(3):421-6. <http://dx.doi.org/10.1002/pssa.200306728>.
43. Sachanyuk VP, Olekseyuk ID, Parasyuk OV. X-ray powder diffraction study of the  $\text{Cu}_2\text{Cd}_{1-x}\text{MnxSnSe}_4$  alloys. *Phys Status Solidi.* 2006;203(3):459-65. <http://dx.doi.org/10.1002/pssa.200521349>.
44. Mora AJ, Delgado GE, Grima-Gallardo P. Crystal structure of  $\text{CuFeInSe}_3$  from X-ray powder diffraction data. *Phys Status Solidi.* 2007;204(2):547-54. <http://dx.doi.org/10.1002/pssa.200622395>.
45. Delgado GE, Mora AJ, Contreras JE, Grima-Gallardo P, Durán S, Muñoz M, et al. Crystal structure characterization of the quaternary compounds  $\text{CuFeAlSe}_3$  and  $\text{CuFeGaSe}_3$ . *Cryst Res Technol.* 2009;44(5):548-52. <http://dx.doi.org/10.1002/crat.200800596>.
46. Delgado GE, Mora AJ, Grima-Gallardo P, Quintero M. Crystal structure of  $\text{CuFe}_2\text{InSe}_4$  from X-ray powder diffraction. *J Alloys Compd.* 2008;454(1-2):306-9. <http://dx.doi.org/10.1016/j.jallcom.2006.12.057>.
47. Delgado GE, Mora AJ, Grima-Gallardo P, Muñoz M, Durán S, Quintero M, et al. Crystal structure of the quaternary compounds  $\text{CuFe}_2\text{AlSe}_4$  and  $\text{CuFe}_2\text{GaSe}_4$  from X-ray powder diffraction. *Bull Mater Sci.* 2015;38(4):1061-4. <http://dx.doi.org/10.1007/s12034-015-0933-9>.